Cloning of an emopamil-binding protein (EBP)-like protein that lacks sterol Δ^8-Δ^7 isomerase activity

Fabian F. MOEBIUS*[1], Barbara U. FITZKY*, Georg WIETZORREK*, Alexander HAIDEKKER†, Andrea EDER* and Hartmut GLOSSMANN*

*Institut für Biochemische Pharmakologie, Peter-Mayr-Strasse 1, A-6020 Innsbruck, Austria, and †Institut für Gerichtliche Medizin, Müllerstrasse 44, A-6020 Innsbruck, Austria

EBP (emopamil-binding protein) is a high-affinity binding protein for [^{3}H]emopamil and belongs to the family of so-called sigma receptors. Mutations that disrupt EBP's 3β-hydroxysteroid sterol Δ^8-Δ^7 isomerase activity (EC 5.3.3.5) impair cholesterol biosynthesis and cause X-chromosomal dominant chondrodysplasia punctata. We identified a human cDNA for a novel EBPL (EBP-like protein) with a calculated mass of 23.2 kDa. Amino acid sequence alignments and phylogenetic analysis revealed that EBPL is distantly related to EBP (31 % identity and 52 % similarity) and found in animals but not in plants. EBPL is encoded by four exons on human chromosome 13q14.2 covering 30.7 kb, and a partially processed EBPL pseudogene was found on 16q21. The EBPL mRNA was expressed ubiquitously and most abundant in liver, lung and kidney. Upon heterologous expression in yeast EBPL had no detectable 3β-hydroxysteroid sterol Δ^8-Δ^7 isomerase and sigma-ligand-binding activity. Nine out of ten amino acid residues essential for catalytic activity of EBP were conserved in EBPL. Replacement of the only differing residue (EBP-Y111W) reduced catalytic activity of EBP. Transfer of the divergent residue from EBP to EBPL (EBPL-W91Y) and chimaerization of EBP and EBPL at various positions failed to restore catalytic activity of EBPL. Chemical cross-linking induced homodimerization of EBPL and EBP. Whereas mevinolin increased the mRNA for EBP and DHCR7 (Δ^7-sterol reductase) in HepG2 cells, it had no effect on mRNAs for EBPL and sigma$_1$ receptor, indicating that EBP and EBPL expression are not co-ordinated. We propose that EBPL has a yet-to-be-discovered function other than cholesterol biosynthesis.

Key words: cholesterol biosynthesis, 3β-hydroxysteroid sterol Δ^8-Δ^7 isomerase, sigma receptor.

INTRODUCTION

We previously characterized, purified and cloned the EBP (emopamil-binding protein), a high-affinity receptor for the phenylalkylamine calcium-antagonist emopamil and other anti-ischaemic drugs (reviewed in [1]). EBP was shown to be an enzyme of post-squalene cholesterol biosynthesis catalysing the shift of a double bond in the B-ring of the sterol nucleus (3β-hydroxysteroid sterol Δ^8-Δ^7 isomerase; EC 5.3.3.5 [2]). The isoenzyme of EBP from yeast, ERG2, is structurally diverse from EBP but is homologous with the sigma$_1$ receptor. This mammalian protein interacts physically and functionally with InsP_3 receptors and K^+ channels [3,4]. Sigma$_1$ receptor, ERG2 and EBP are all high-affinity binding proteins for the sigma ligand [^{3}H]ifenprodil [5]. The pharmacological commonalities of EBP and ERG2 with sigma$_1$ and sigma$_2$ receptors suggested that EBP also belonged to the family of so-called sigma receptors [1]. EBP is localized on chromosome Xp11.23–p11.22 and is essential for cholesterol biosynthesis. Mutations in *EBP* cause X-chromosomal dominant chondrodysplasia punctata {CDPX2; OMIM (Online Mendelian Inheritance in Man) no. 302960 [6,7]}, a rare disease that is lethal in most males (for exceptions see [8,9]) and affects patches of skin and bone in females due to random X-inactivation and Lyonization (reviewed in [10]). Because of the pharmacological relationship of EBP with sigma$_2$ receptors and the similarity of the mass of the photoaffinity-labelled sigma$_2$ receptor of 18–22 kDa to that of EBP [11], we hypothesized that the sigma$_2$ receptor would be structurally similar to either EBP or the sigma$_1$ receptor. We therefore searched vertebrate DNA databases for proteins homologous to EBP or sigma$_1$ receptor. A TBLASTN search in the EST database with the EBP amino acid sequence as a template identified novel cDNA fragments encoding a protein that is related to EBP in its amino acid sequence and putative topology as a sigma$_2$-receptor candidate protein.

Here we characterize this novel EBPL (EBP-like protein) and demonstrate that, unlike EBP, when expressed in 3β-hydroxysteroid sterol Δ^8-Δ^7 isomerase-deficient yeast cells EBPL has no detectable catalytic activity. Moreover EBPL does not bind sigma ligands such as [^{3}H]ifenprodil, [^{3}H]ditolylguanidine or [^{3}H]haloperidol with high affinity, suggesting that it does not form the long-sought sigma$_2$-ligand-binding site. Endogenous EBPL predominantly forms homodimers and associates only weakly with EBP upon heterologous expression. EBPL expression is not regulated by inhibition of cholesterol biosynthesis at the level of HMG-CoA reductase (3-hydroxy-3-methylglutaryl-CoA reductase).

EXPERIMENTAL

Molecular cloning

Partial human cDNA clones (GenBank® accession nos. H49343, W78859 and W84713) were identified with the TBLASTN algorithm because of their amino acid sequence homology with EBP (GenBank accession no. Z37986) in the EST database, obtained from the Resource Center/Primary Database (RZPD, Berlin, Germany) and resequenced. The 5′ end of the EBPL cDNA was amplified using Marathon-Ready cDNA (Clontech) from human

Abbreviations used: DHCR7, Δ^7-sterol reductase; EBP, emopamil-binding protein; EBPL, EBP-like protein; RACE, rapid amplification of cDNA ends; HMG-CoA reductase, 3-hydroxy-3-methylglutaryl-CoA reductase.

[1] To whom correspondence should be addressed (e-mail Fabian.Moebius@uibk.ac.at).

The reported sequences have been deposited in the GenBank® Nucleotide Sequence Database under accession nos. AF243433 and AF243434.

liver and the antisense oligonucleotide 5′-CAGAGACCCATCCAGGGCGACG-3′. The full-length cDNA was constructed in pBluescript SK using the clone corresponding to GenBank acession no. W78859 and the RACE (rapid amplification of cDNA ends) PCR product. The 5′ end of mouse Ebpl cDNA was amplified by RACE PCR using the antisense oligonucleotide 5′-AAGATGCAATCAAGCCTTGGG-3′ with cDNA transcribed from total mouse liver RNA with the 5′ RACE kit (Gibco-BRL) and assembled with the 3′ end of the clone corresponding to GenBank acession no. W66616. DNA sequencing of both strands was carried out according to standard procedures. Multiple amino acid sequences were aligned with CLUSTALW version 1.81 (http://www.cmbi.kun.nl/bioinf/tools/clustalw.shtml) and phylogenetic trees were calculated with PHYLIP (http://www.genebee.msu.su/services/phtree_reduced.html). The hydropathy of the amino acid sequence was analysed according to Kyte and Doolittle [12] with a window size of 19 (http://bioinformatics.weizmann.ac.il/hydroph/cmp_hydph.html).

Northern blots

A human multiple-tissue Northern blot (Clontech) was hybridized with a ^{32}P-labelled probe corresponding to the entire cDNA of EBPL. Multiple-tissue Northern dot blots (Clontech) were probed with ^{32}P-labelled cDNAs corresponding to human EBPL, EBP, DHCR7 (Δ^7-sterol reductase) and the sigma$_1$ receptor (GenBank accession nos. AF243433, Z37986, AF034544 and U79528, respectively). To analyse regulation of EBPL mRNA, HepG2 cells were treated in the absence or presence of 1 μM mevinolin and 1 μM 25-hydroxycholesterol (Sigma–Aldrich) for 2 days in 10 % lipid-depleted serum [13] in RPMI 1640. Total RNA (15 μg) was extracted with RNeasy (Qiagen, Hilden, Germany), separated by agarose-gel electrophoresis and hybridized subsequently with ^{32}P-labelled probes corresponding to the open reading frames of EBPL, EBP, sigma$_1$ receptor and DHCR7 and the cDNA for the human transferrin receptor (Clontech). Hybridization signals were analysed quantitatively with a FujiX Bas 1000 Phosphorimager and the program TINA and normalized to human transferrin receptor mRNA.

Heterologous expression

For heterologous expression the 5′ and 3′ non-coding sequences of the EBPL cDNA were replaced with *Xho*I and *Not*I restriction sites (EBPL). An N-terminal c-Myc epitope tag preceded by an *Xho*I site was added by PCR (mycEBPL). Protein expression in yeast strain WA0 (*α his7-2 leu2-3,112 ura3-52 erg2-3*) was carried out as described previously using the 2 micron yeast expression plasmid Yep351ADC1 [14]. EBPL was expressed in tsA201 cells by subcloning into pCIneo (Promega) and transfection with $CaCl_2$ as described in [15]. Point mutations were introduced into the EBP and EBPL cDNA by PCR as described in [16]. The following chimaeric proteins were created by PCR in evolutionarily conserved amino acid residues: mycEBP-Y104-EBPL (where the N-terminus is Myc-epitope-tagged EBP and the C-terminus is EBPL; chimaerized at Tyr-104 of EBP and Tyr-84 of EBPL, respectively), mycEBP-T125-EBPL (chimaerized at Thr-125 of EBP and Thr-105 of EBPL, respectively), mycEBP-W196-EBPL (chimaerized at Trp-196 of EBP and Trp-176 of EBPL, respectively), mycEBPL-Y84-EBP (where the N-terminus is Myc-epitope-tagged EBPL and the C-terminus is EBP; chimaerized at Tyr-84 of EBPL and Tyr-104 of EBP, respectively) and mycEBPL-E58-EBP (chimaerized at Glu-58 of EBP and Glu-80 of EBPL, respectively). Construct integrity was verified by automated DNA sequencing.

Miscellanous

Antibodies against a synthetic peptide LIASLWKEYGKAD corresponding to amino acid residues 76–88 of EBPL were raised in rabbits (ERP1, S180) and affinity purified as described in [17]. For immunoprecipitation microsomes were prepared from tsA201 cells 2 days after transfection by homogenization in 25 mM Tris/HCl, pH 7.5, 5 mM EDTA, 0.1 mM PMSF and 0.1 mM benzamidine at 4 °C, and ultracentrifugation of the homogenate after removal of non-lysed cells. Solubilized microsomal proteins (100 μg) in 0.1 % (w/v) digitonin, 0.15 M NaCl, 25 mM Tris/HCl, pH 7.5, and 0.1 mM PMSF at 4 °C were incubated with 10 μl of crude anti-EBPL (αEBPL) serum conjugated to Protein A–Sepharose (Sigma–Aldrich). After washing, Sepharose-bound proteins were eluted with SDS sample buffer containing 10 mM dithiothreitol and analysed by SDS/PAGE and immunoblotting. Cross-linking of solubilized microsomal proteins was carried out in 1 % (w/v) digitonin, 0.1 M NaCl, 0.05 M Na_2HPO_4/NaH_2PO_4, pH 8, by adding glutaraldehyde at the concentrations indicated for 2 h at 4 °C. Cross-linking was stopped with SDS sample buffer containing 10 mM dithiothreitol. Immunoblotting with anti-c-Myc antibody (αc-Myc; Calbiochem; final concentration, 0.05 μg/ml), αEBPL (final concentration, 0.5 μg/ml), anti-EBP antibody (αEBP; corresponding to residues 2–26 of guinea pig EBP [17]; final concentration, 0.2 μg/ml), anti-(sigma$_1$ receptor) antibody (αsigma$_1$ receptor; corresponding to residues 142–166 of guinea pig sigma$_1$ receptor [18]; final concentration, 0.1 μg/ml), sterol analysis and [^{3}H]ifenprodil, [^{3}H]haloperidol, [^{3}H]ditolylguanidine and [^{3}H]emopamil binding were carried out as described in [5,17]. Sterols were analysed by UV spectroscopy and GC/MS as described in [16].

Immunocytochemistry

HepG2 and tsA201 cells were grown on gelatin/polylysine-coated coverslips and co-transfected with 2 μg of mycEBP- and EBPL-pCIneo per 6-cm culture dish using Fugene 6 (Roche, Wien, Austria). After 48 h transfected cells were fixed with 4 % (w/v) paraformaldehyde/4 % (w/v) sucrose in PBS for 20 min and subsequently lysed with concentrated methanol for 10 min. After blocking for 30 min with 5 % (v/v) normal goat serum in 0.2 % (w/v) Triton X-100/0.02 % (w/v) BSA in PBS (TRI/BSA/PBS), αc-Myc (final concentration, 0.05 μg/ml) and αEBPL (final concentration, 0.25 μg/ml) antibodies were added in TRI/BSA/PBS overnight at 4 °C. After washing, fluorochrome-conjugated secondary antibodies were added at 0.5 μg/ml (goat anti-mouse Alexa 488 and goat anti-rabbit Alexa 594; Molecular Probes, Eugene, OR, U.S.A.). No immunofluorescence was observed in mock-transformed cell lines or when primary antibodies were omitted. As a control for endoplasmic-reticulum expression cells were transfected with pEYFP-ER (Clontech). After embedding in 3 mg/ml *p*-phenylenediamine, slides were analysed with an Axioplan 2 microscope equipped with an Axiocam digital camera and Axiovision image-analysis software (Zeiss, Oberkochen, Germany).

RESULTS

Molecular cloning of EBPL

To identify novel EBPL proteins we screened the EST database with the amino acid sequence of EBP and identified several cDNAs from human and murine tissues encoding parts of a protein that was distantly related to EBP. Full-length cDNAs of EBPL from human and mouse were constructed by amplifying

the 5′ end of the cDNA with RACE, which was impeded by a 90 % GC content of the 5′ coding sequence (bp 53–130 of the EBPL open reading frame) and resulted in the assembly of 913- and 838-bp cDNA sequences of human EBPL and mouse Ebpl, respectively. Screening of a guinea pig cDNA library with PCR identified a partial EBPL-encoding cDNA (results not shown). A putative polyadenylation sequence (AATAAA) was identified at position 843–848 of the human cDNA sequence, indicating that the 3′ untranslated region is complete. The longest open reading frames of human and mouse cDNAs encoded 204-amino-acid proteins with calculated masses of 23.2 and 23.3 kDa respectively that were 75 % identical and 83 % similar over their entire length. Even so, EBPL differed from EBP by having a 20-amino-acid-shorter N-terminus. The open reading frame was probably identified correctly because in SDS/PAGE gels migration of the recombinant protein expressed from the open reading frame without 5′ and 3′ untranslated region was indistinguishable from migration of the native microsomal protein (see below). The hydropathy profile of EBPL analysed with the algorithm of Kyte and Doolittle [12] (window size 19) was very similar to that of EBP [14] (results not shown) and predicted four putative transmembrane segments. EBP and EBPL were 31 % identical and 52 % similar over 172 amino acid residues comprising transmembrane segments 2–4 with the N- and C-termini showing no similarity. The BLASTN algorithm found no significant similarity between EBP and EBPL at the nucleotide level. As in EBP the C-terminus in EBPL encoded a putative sequence for retention of type I integral membrane proteins in the endoplasmic reticulum. This sequence motif, which consists of several lysine residues [19], is less obvious in EBPL (KETSSVKKFQ) than in EBP (KATKAKSKKN). An *in silico* screen of the EST database with the EBPL sequence as a template identified several EST sequences encoding EBPL-related proteins from rat, *Xenopus laevis* and fish, but none from plants.

To clarify the phylogenetic relationship between EBP and EBPL, we searched for additional EBP-related proteins from other species with the amino acid sequences of EBP from human and *Arabidopsis thaliana* [20] as templates. This resulted in the identification of cDNAs encoding EBP-related proteins from plants, vertebrates and green algae, but not from worms or flies. The alignment of a 134-amino-acid sequence fragment (Figure 1, top panel) and subsequent phylogenetic analysis (Figure 1, bottom panel) of the available partial and complete sequences of EBP-related proteins with PHYLIP [21] revealed four distinct groups. Whereas all plant sequences fell into one group in which the evolutionary relationship between various plant species was reproduced, the only sequence from green algae available formed a separate group, reflecting the early separation of plants and green algae [22]. Sequences of EBP-related proteins from vertebrates such as human, zebrafish and *X. laevis* formed two groups of EBP- and EBPL-related protein sequences. Sequences of EBP-related proteins from plants were more similar to vertebrate EBP than EBPL, indicating that all available cDNA sequences from plants encode orthologues of EBP and that EBPL is absent from plant genomes.

Cloning of the *EBPL* gene

To compare the structure of *EBP* and *EBPL* genes, we searched the GenBank database for genomic sequences encoding EBPL. Comparison of the organization of the 30.7 kb *EBPL* gene (Table 1), as derived from sequence with accession no. AL135901 (clone ID RP11-432M24), with that of the 6.9-kb *EBP* gene [7] revealed that the coding regions of *EBP* and *EBPL* contained three introns, while a fourth intron was found in the 5′ untranslated region of EBP. All introns bar one were in different positions in the EBP and EBPL amino acid sequences. This conserved intron was localized in amino acid residues Trp-81 of EBPL and Trp-101 of EBP, respectively (Figure 1, top panel). Intron–exon boundary sequences of the four exons of *EBPL* conformed to the consensus sequences described [23]. The sizes of introns 2 and 3, of 6.6 and 1.8 kb, were confirmed by PCR, whereas no PCR product was obtained from intron 1 in line with its size of > 20 kb. The nucleotide sequences of the EBPL cDNA and the exons of the *EBPL* gene were completely identical. The genomic clone RP11-432M24 comprised the sequence-tagged sites D13S862E and D12S273, which were 10 and 45 kb respectively upstream from *EBPL*. The sequence from accession no. AL135901 was part of the 55-Mbp contig NT_024524, overlapped with the flanking clones AL139321 and AL136123 and was assigned to chromosome 13q14.2 by the International Human Genome Sequencing consortium (http://www.ensembl.org). In addition to the complete *EBPL* gene on chromosome 13 we identified a partially processed pseudogene in sequence AC093536 (clone ID RP11-744D14) corresponding to nucleotides 124–913 of the EBPL full-length cDNA sequence. The *EBPL* pseudogene contained 121 bp of intron 1 sequence, multiple missense, frameshift and nonsense mutations and six nucleotides of a putative poly(A)$^+$ tail. Genomic clones encoding the pseudogene were assigned to chromosome 16q21 by the International Human Genome Sequencing consortium. Phylogenetic analysis of the pseudogene revealed a close similarity to human EBPL (results not shown) suggesting an evolutionarily recent integration of an incompletely processed EBPL mRNA. No EST sequences originating from this pseudogene were identified in GenBank.

Tissue distribution of EBPL mRNA

In Northern blots with mRNA from human heart, brain, lung, liver, skeletal muscle, kidney and pancreas a 1.1 kb EBPL transcript was expressed ubiquitously (results not shown). Multiple-tissue dot blots with total human RNA confirmed the ubiquitous expression of EBPL, with the highest densities being present in liver, lung and kidney (Figure 2). However, most other human tissues (Figure 2) and cell lines (results not shown) also contained substantial amounts of EBPL mRNA. A comparison of the tissue-distribution profile of EBPL mRNA with that of the human sigma$_1$ receptor and the sterol-biosynthesizing enzymes EBP (Figure 2) and DHCR7 (results not shown) revealed that the tissue distribution of the EBPL mRNA was similar to that of the sigma$_1$ receptor, except for the higher density of the sigma$_1$ receptor mRNA in brain (Figure 2).

Heterologous expression of EBPL and identification of the endogenous protein

To verify that the cloned cDNA encoded full-length EBPL, we expressed the open reading frame with and without an N-terminal c-Myc epitope tag in yeast (*Saccharomyces cerevisiae* strain WA0) and in immortalized human kidney cells (tsA201). Immunoblotting with αc-Myc identified a 22-kDa recombinant protein that migrated faster than EBP in SDS/PAGE, as expected from the calculated molecular masses of EBP and EBPL of 26.4 and 23.2 kDa, respectively (Figure 3, bottom panel). To identify endogenous EBPL we generated affinity-purified polyclonal antibodies (αEBPL) against a synthetic peptide corresponding to the EBPL sequence. αEBPL cross-reacted with c-Myc-tagged as well as with non-tagged recombinant EBPL, but not with EBP (Figure 3, top panel). The migration of the non-tagged recombinant protein was indistinguishable from immunoreactive

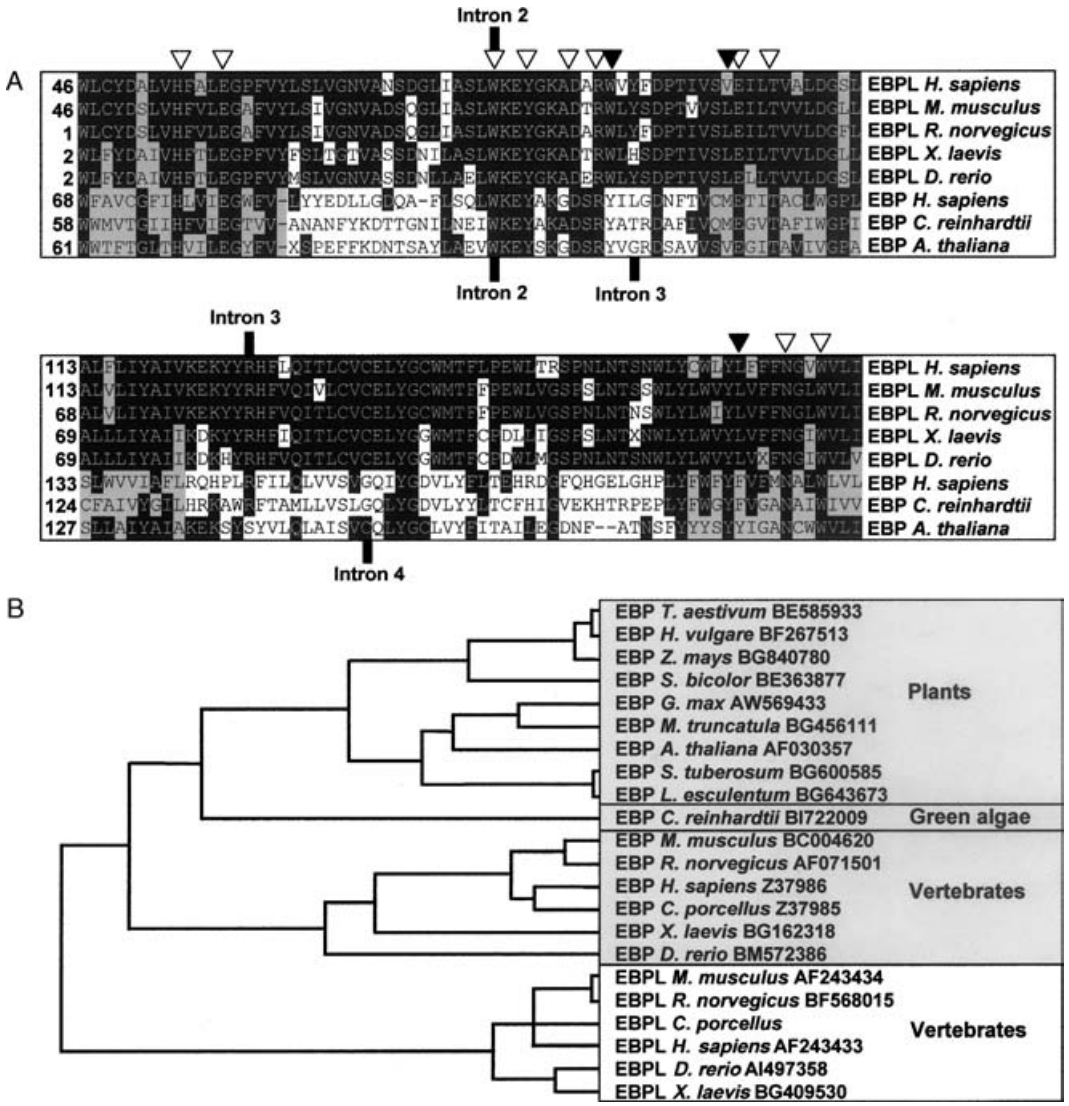

Figure 1 Amino acid sequence alignment and phylogenetic tree analysis

(**A**) Amino acid sequence alignment of EBPL from vertebrates and EBP from humans (*Homo sapiens*), green algae (*Chlamydomonas reinhardtii*) and plants (*A. thaliana*). Amino acid sequences from the indicated sources were aligned with CLUSTALW. Numbers on the left refer to amino acid sequence positions. Black boxes highlight residues identical in the majority of sequences. Grey boxes indicate putative transmembrane segments II–IV of EBP and EBPL. Positions and numbering of introns are shown for EBPL (upper lines) and EBP (lower lines) respectively. Open triangles indicate amino acid residues required for catalytic activity (less than 10 % of wild type $\Delta^{5,7}$-sterol formation [16]). Black triangles show EBPL amino acid residues introduced into the EBP sequence by site-directed mutagenesis. (**B**) Phylogenetic tree calculated by PHYLIP from a CLUSTALW version 1.81 alignment of amino acid residues 46–176 of EBPL with sequences of EBP from the indicated species (GenBank cDNA accession nos. are shown). Species used in (**A**) and (**B**) are *Mus musculus*, *Rattus norvegicus*, *Danio rerio*, *Triticum aestivum*, *Hordeum vulgare*, *Zea mays*, *Sorghun bicolor*, *Glycine max*, *Medicago trunculata*, *Solanum tuberosum*, *Lycopersicon esculentum* and *Cavia porcellus*.

Table 1 Intron–exon organization of *EBPL*

Intron	cDNA position	Exon sequence	5′ Intron sequence	Intron length (bp)	3′ Intron sequence	Exon sequence
1	171	GCGCTG	gtaagtgcca	21 408	tcctctctag	GAAGGC
2	241	CTTTAT	gtaagtaatt	6582	ttgtctttag	GGAAAG
3	380	TTACCG	gtaggtgccc	1849	tctccaacag	GCATTT

bands in microsomes from immortalized human hepatocytes (HepG2 cell line; Figure 3, top panel) and mouse (Figure 3, top panel) and guinea pig liver (results not shown). This demonstrated that EBPL was indeed expressed in humans and mice and that the cDNA encoded full-length EBPL. The intensities of α c-Myc-immunoreactive EBP and EBPL bands upon heterologous expression (Figure 3, bottom panel) were similar. Since the same holds true for the recombinant EBP and EBPL proteins from HepG2 cells (Figure 3, top and middle panels) and liver microsomes detected with αEBPL and αEBP, respectively, we estimated that EBP and EBPL were expressed at similar steady-state protein levels.

Functional analysis of EBPL

The amino-acid sequence homology between EBP and EBPL prompted us to investigate whether EBPL is catalytically active. 3β-Hydroxysteroid sterol Δ^8-Δ^7 isomerase activity of EBP can be determined by heterologous expression in the isomerase-deficient

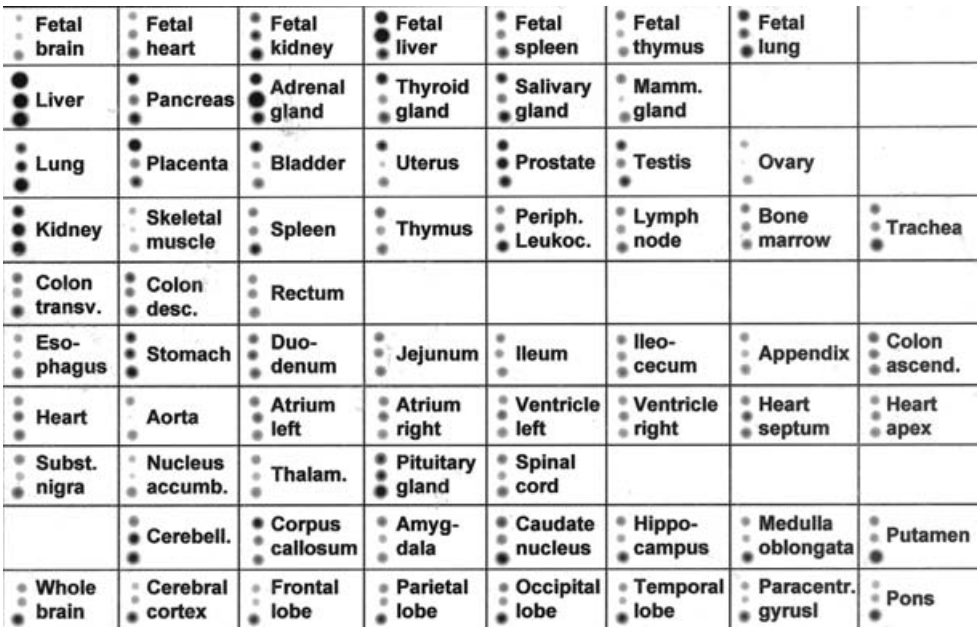

Figure 2 Northern dot-blot analysis of EBPL steady-state mRNA levels

A human multiple tissue expression array 2 (Clontech; lot no. 0010076) loaded with poly(A)$^+$ RNA normalized to eight different housekeeping genes was hybridized sequentially with ^{32}P-labelled cDNA probes corresponding to EBPL, EBP and sigma$_1$ receptor, respectively, and exposed to X-ray film. After each hybridization the blot was stripped as described in the manufacturer's user manual and complete removal of radiolabelled probe was verified by re-exposure to X-ray film. Dot intensity was normalized to liver. Dots represent EBPL (top), EBP (middle) and sigma$_1$ receptor (bottom).

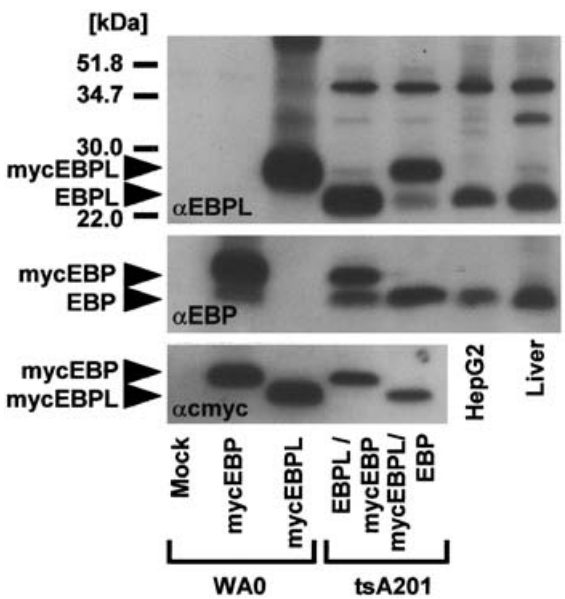

Figure 3 Immunoblot analysis of heterologously expressed and endogenous EBPL

Microsomal proteins from yeast (strain WA0; 5 μg of protein/lane) and human embryonic kidney cells (tsA201; 10 μg of protein/lane) expressing c-Myc-epitope-tagged EBP and EBPL (mycEBP, mycEBPL) and the open reading frame without tag (EBP, EBPL), or from immortalized human liver cells (HepG2; 50 μg/lane) or mouse liver microsomes (liver; 50 μg/lane), respectively, were separated by SDS/PAGE and analysed with antibodies against the c-Myc epitope tag, EBP and EBPL. One of several experiments giving identical results is shown.

yeast strain WA0, in which ERG2, the endogenous 3β-hydroxysteroid sterol Δ^8-Δ^7 isomerase of yeast, is mutated (erg2-3 mutation [24]). Sterols can be identified by either GC/MS or spectrophotometric measurement of UV-absorbing $\Delta^{5,7}$-sterols such as ergosterol formed only when the 3β-hydroxysteroid sterol Δ^8-Δ^7 isomerase is active [16]. In contrast with EBP, EBPL failed to complement the erg2–3 mutation when the sterol composition was analysed either spectrophotometrically (Figure 4A) or by GC/MS (results not shown). EBPL expression was verified by immunoblotting and found to be comparable with EBP (Figure 3). Since we hypothesized originally that EBPL formed the sigma$_2$ receptor, we also measured the ability of EBPL to bind high-affinity sigma ligands. However, EBPL failed to bind [^{3}H]ifenprodil (Figure 4B), [^{3}H]emopamil, [^{3}H]haloperidol, (+)-[^{3}H]pentazocine and [^{3}H]ditolylguanidine (results not shown), indicating that upon heterologous expression in yeast EBPL does not form the sigma$_2$ receptor. To ascertain that a lack of catalytic activity was not due to reduced protein expression, we verified EBPL expression by immunoblotting (Figure 4C). To rule out a lack of activity being attributable to the N-terminal c-Myc tag we expressed EBPL without the epitope tag, which also failed to complement the erg2–3 mutation (results not shown).

In a previous study of EBP we had identified ten residues that were indispensable for EBP-mediated catalysis and several residues that were required for high-affinity [^{3}H]ifenprodil binding [16]. Failure of EBPL to bind [^{3}H]ifenprodil and to catalyse sterol isomerization prompted us to inspect the amino acid sequence of EBPL for amino acid residues that we had identified previously in EBP as being required for catalysis [16] that were not conserved in EBPL. We identified two residues (Met-121, Phe-189) that in EBP upon substitution with Ala reduced the catalytic activity and one residue (Tyr-111) that caused a complete loss of function of EBP when replaced with Ala. To assess the role of Tyr-111, Met-121 and Phe-189 in EBP-mediated catalysis, we mutated these residues into the corresponding residues of EBPL (Y111W, M121V and F189L) and expressed mutant EBP proteins in 3β-hydroxysteroid sterol Δ^8-Δ^7 isomerase-deficient yeast strain WA0. We observed previously that EBP-mediated

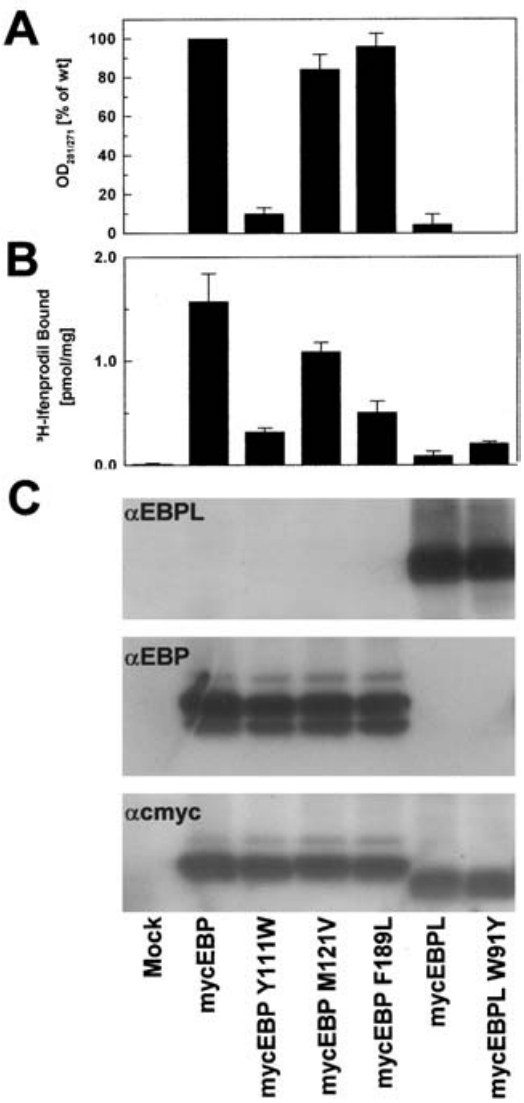

Figure 4 Heterologous expression and functional analysis of EBPL in yeast strain WA0

(**A**) Formation of UV-absorbing $\Delta^{5,7}$-sterols by yeast strains transformed with cDNAs encoding the indicated wild-type and mutant proteins. Sterols were extracted and quantified by spectrophotometry. Data (means ± S.D., $n = 4$–20) were normalized to extracts from mycEBP- (100 %) and mock- (0 %) transformed strains, respectively. (**B**) [^{3}H]Ifenprodil-binding activity in microsomes from yeast strains expressing the indicated proteins. Binding activity was normalized to microsomal protein concentrations (means ± S.D., $n = 3$). (**C**) Immunoblot analysis of protein expression. Microsomal proteins (5 μg/lane) were separated by SDS/PAGE and subjected to immunostaining with the indicated antisera. One of several experiments giving identical results is shown.

formation of $\Delta^{5,7}$-sterols was not linear with protein expression, so that a 50-fold reduction of expression resulted only in a 6.5-fold decrease in $\Delta^{5,7}$-sterols [16]. Whereas the EBP-M121V and EBP-F189L mutations had no major effects on catalytic activity, the formation of UV-absorbing $\Delta^{5,7}$-sterols by the EBP-Y111W mutant was decreased 10-fold, which suggested that the catalytic activity of EBP-Y111W was less than 2 % of the wild type. We also observed substantially reduced [^{3}H]ifenprodil-binding activity of this mutant (Figure 4B). To test whether the lack of catalytic activity of EBPL was due to a single amino-acid substitution we mutated Trp-91, the amino acid residue of EBPL corresponding to Tyr-111 of EBP, into Tyr. Even so, EBPL-W91Y was catalytically inactive in yeast; this mutant specifically bound [^{3}H]ifenprodil (Figure 4B), albeit with a higher dissociation rate constant than EBP (results not shown).

To test whether the lack of catalytic activity of EBPL resided in more than one amino-acid substitution, we chimaerized EBP and EBPL at various positions, putting either the EBP or the EBPL sequence at the N-terminus preceded by a c-Myc epitope tag (see the Experimental section). None of the five chimaeric proteins had detectable 3β-hydroxysteroid sterol Δ^8-Δ^7 isomerase- and [^{3}H]ifenprodil-binding activity; even so, all were expressed in yeast (results not shown). The affinity-purified polyclonal antibodies raised against amino acid residues 76–88 of EBPL were highly specific for EBPL and showed no detectable cross-reactivity with EBP (Figure 3 and 4C). Surprisingly, these antibodies cross-reacted with chimaera mycEBP-Y104-EBPL (results not shown), chimaerized within the immunogenic peptide at Tyr-84 (underlined below). In this chimaera the first eight antigenic amino acid residues came from EBP, suggesting that the specificity of the antibodies for EBPL is based upon discrimination of the Y**G**K**A**D sequence of EBPL from the Y**A**K**G**D sequence of EBP. To rule out the lack of catalytic activity and radioligand binding being due to recent mutations in EBPL, we also cloned and heterologously expressed the murine Ebpl cDNA, but found neither 3β-hydroxysteroid sterol Δ^8-Δ^7 isomerase activity nor sigma-ligand binding {[^{3}H]haloperidol, [^{3}H]ifenprodil, [^{3}H]ditolguanidine and (+)-[^{3}H]pentazocine; results not shown}.

EBPL does not dimerize quantitatively with EBP

Failure of EBPL to complement isomerase-deficient yeast raised the possibility that EBPL required association with EBP to function. To test whether EBPL was physically associated with EBP, we immunoprecipited EBPL with αEBPL and analysed the immunoprecipitate for EBPL- and EBP-associated c-Myc immunoreactivity. Immunoprecipitation of recombinant EBPL was saturable and quantitative (Figure 5A), but required αEBPL serum, since affinity-purified antibodies failed to immunoprecipitate EBPL quantitatively (results not shown). Specificity was demonstrated by the lack of immunoprecipitation by the αEBPL preimmune serum (Figure 5B). Since both the αEBP and the αEBPL sera were raised in rabbits and the molecular masses of EBP and EBPL are very similar to that of the immunoglobulin light chain, we used a primary antibody from mouse directed against the c-Myc epitope for detection of co-immunoprecipitated EBP. Both proteins were co-expressed in immortalized human kidney cells (tsA201). αEBPL serum precipitated EBPL quantitatively (Figure 5B), but only a small fraction of EBP co-immunoprecipitated, suggesting a weak interaction, if any, between EBP and EBPL. Since we could not rule out that EBP and EBPL interacted only weakly and quickly dissociated upon immunoprecipitation, we exploited our previous observation that the apparent migration of EBP in SDS/PAGE gels decreased upon cross-linking with glutaraldehyde [17]. This decrease in relative migration corresponded approximately to a duplication of the mass, suggesting that glutaraldehyde cross-linked EBP monomers and caused dimerization. However, because of the similar migration of EBP and EBPL in SDS/PAGE gels, we could not rule out that our previous results were attributable to glutaraldehyde-cross-linked EBP–EBPL heterodimers instead of EBP homodimers. We therefore incubated digitonin-solubilized microsomes with glutaraldehyde and analysed them for EBPL and EBP immunoreactivity. We reasoned that if EBP and EBPL formed a heterodimer the migration of αEBP- and αEBPL-immunoreactive bands should become indistinguishable upon

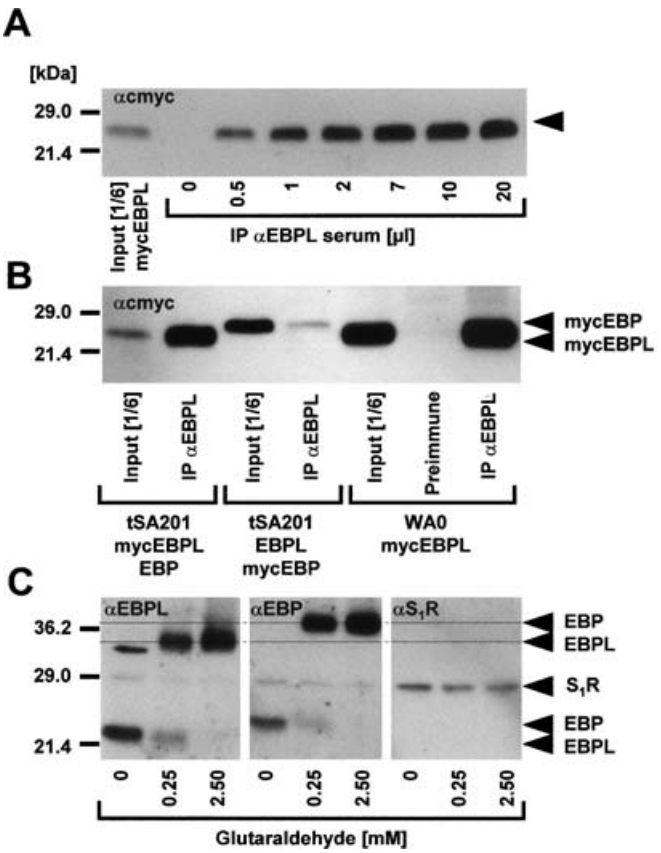

Figure 5 Immunoprecipitation of EBPL

(**A**) Immunoprecipitation of recombinant mycEBPL. Increasing volumes of αEBPL serum were incubated with 1 %-(w/v)-digitonin-solubilized microsomes from yeast overexpressing mycEBPL. Input was one-sixth of the material subjected to immunoprecipitation. (**B**) Co-immunoprecipitation of recombinant mycEBP with EBPL. Microsomes from tsA201 cells transfected with combinations of either mycEBP/EBPL or EBP/mycEBPL were solubilized with 1 % (w/v) digitonin and incubated with αEBPL serum. Immunoprecipitated proteins were analysed by SDS/PAGE and c-Myc staining. One of several experiments giving identical results is shown. (**C**) Cross-linking of microsomes from an immortalized liver cell line (HepG2) with glutaraldehyde. 1 %-(w/v)-Digitonin-solubilized microsomes were incubated with the indicated concentrations of glutaraldehyde. The reaction was stopped by the addition of sample buffer and samples were analysed by SDS/PAGE and immunostaining with affinity-purified αEBPL, αEBP and αsigma$_1$-receptor (S_1R) antibodies. αEBPL and αEBP stainings were spiked with αsigma$_1$-receptor antibodies.

dimerization. As negative controls we used the sigma$_1$ receptor which we have demonstrated previously by radiation inactivation analysis to form a functional monomer [18]. Sigma$_1$ receptor (Figure 5C) and DHCR7, the human Δ^7-sterol reductase (results not shown), displayed no reduced migration upon glutaraldehyde cross-linking, indicating that cross-linking was specific for EBP and EBPL. In line with the hypothesis that EBP and EBPL did not heterodimerize, the apparent molecular masses of cross-linked endogenous EBP and EBPL proteins were different (Figure 5C), suggesting that EBP and EBPL predominantly formed homodimers. To rule out that dimerization resulted from association with a third protein, we confirmed our cross-linking results with recombinant EBP and EBPL expressed individually in yeast (results not shown).

Subcellular co-localization of EBP and EBPL

Like EBP, the EBPL sequence contained an C-terminal poly-lysine-rich sequence motif which supposedly retains proteins

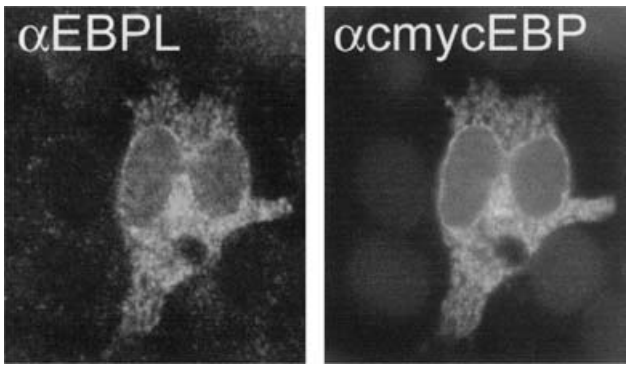

Figure 6 EBP and EBPL share the same subcellular localization

The open reading frames of EBPL and mycEBP were co-transfected into HepG2 cells and stained with αEBPL (left-hand panel) and αc-Myc (right-hand panel), respectively. Secondary antibodies labelled with Alexa 594 (left-hand panel) and Alexa 488 (right-hand panel) were used for detection. A granular distribution of EBPL and EBP immunoreactivities across the cytoplasm and strong perinuclear but no plasmalemmal staining were observed. The same distributions were observed in non-dividing cells. Micrographs from one of several experiments giving identical results are shown.

in the endoplasmic reticulum [19]. To investigate whether EBPL shared the reported perinuclear and endoplasmic-reticulum localization of EBP [25], we heterologously co-expressed Myc-tagged EBP and native EBPL in immortalized human renal and hepatic cell lines (tsA201 and HepG2). Immunostaining with α c-Myc and αEBPL showed identical distributions of immunofluorescence of mycEBP and EBPL, respectively (Figure 6). A similar pattern was seen when cells were transfected with a fluorescent marker protein (enhanced yellow fluorescent protein, EYFP) with an endoplasmic-reticulum-targeting sequence (EYFP-ER; results not shown), suggesting that EBPL shares the subcellular localization of EBP in the endoplasmic reticulum.

No response of EBPL mRNA to inhibition of sterol metabolism

EBP and DHCR7 are enzymes of sterol metabolism which are regulated by sterol-responsive elements [26,27]. To test whether EBPL also responded to inhibition of sterol metabolism with increased transcription we treated HepG2 cells with mevinolin and 25-hydroxycholesterol in the absence of cholesterol and analysed the steady-state mRNA levels of EBPL, EBP, DHCR7 and sigma$_1$ receptor in total RNA from cells treated for 2 days (Figure 7). Mevinolin inhibits HMG-CoA reductase, the key enzyme of cholesterol biosynthesis and deprives cells of cholesterol, resulting in the induction of sterol biosynthetic enzymes. 25-Hydroxycholesterol inhibits transcription of sterol regulated genes by an unknown mechanism. Whereas both treatments had the expected effect of increased and decreased steady-state mRNA levels of DHCR7 and EBP, respectively, they had no significant effect on the steady-state mRNA levels of EBPL and sigma$_1$ receptor. This suggested that EBPL and sigma$_1$ receptor were both not regulated by sterols.

DISCUSSION

Vertebrate EBP and yeast ERG2 have in common 3β-hydroxysteroid sterol Δ^8-Δ^7 isomerase activity and similar pharmacological properties, but have no similarity in their amino acid sequences or hydropathy plots [1]. The sigma$_1$ receptor, despite being pharmacologically and structurally related to ERG2 (30 %

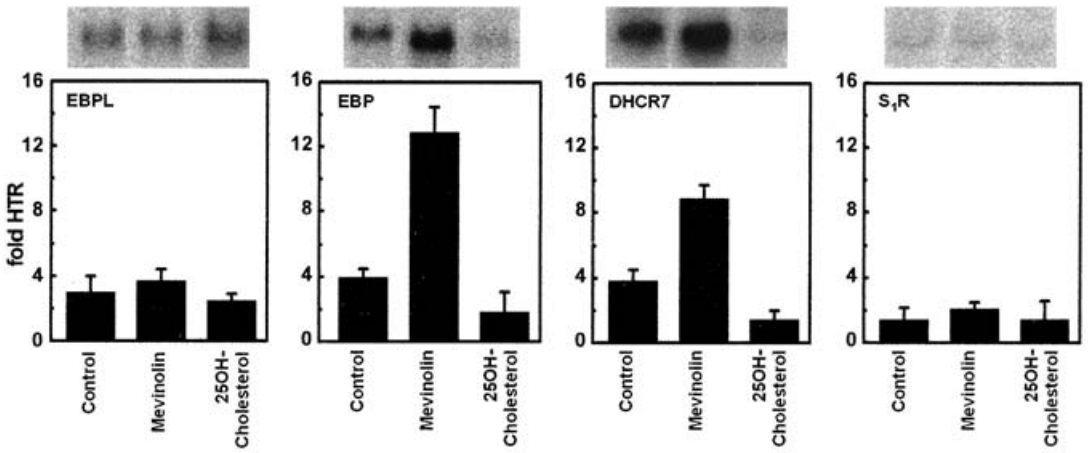

Figure 7 Induction of EBP and DHCR7 but not EBPL mRNA by inhibition of sterol metabolism

HepG2 cells were treated with 1 μM mevinolin and 1 μM 25-hydroxycholesterol in cholesterol-deprived medium. Total RNA was extracted after 2 days of treatment and 15 μg of RNA was analysed by Northern blotting with ^{32}P-labelled probes for human EBPL, EBP, DHCR7 and sigma$_1$ receptor (S_1R). Human transferrin receptor mRNA was used as a loading control. Intensities were quantified with a Phosphorimager and normalized relative to the human transferrin receptor mRNA (HTR). Data shown are the means $\pm$ S.D. ($n = 4$). Only mevinolin-induced expression of EBP and DHCR7 mRNA was significantly different from control ($P < 0.001$).

identity, 66% homology, similar hydropathy plot), has no 3β-hydroxysteroid sterol Δ^8-Δ^7 isomerase activity when expressed in yeast [18]. Here we describe EBPL, a protein that is structurally related to EBP but has neither affinity for radiolabelled sigma ligands nor catalytic activity in yeast. The phylogenetic analysis of the EBP and EBPL amino acid sequence alignment revealed that the EBP-related proteins from plants and green algae are more closely related to EBP than to EBPL and that EBPL is expressed only in vertebrates. As expected, no EBP-related proteins were found in the genomes of *Caenorhabditis elegans* or *Drosophila*, which lack the ability to synthesize sterols. Possible interpretations of this phylogenetic tree are that *EBPL* originated from a duplication of the ancestral 3β-hydroxysteroid sterol Δ^8-Δ^7 isomerase gene which predated the split between vertebrates and plants and that the duplicated gene got lost in plants and green algae but not in vertebrates. Alternatively, *EBPL* might be the result of a duplication of EBP/3β-hydroxysteroid sterol Δ^8-Δ^7 isomerase soon after the evolutionary split of vertebrates from plants. Duplicated genes are redundant and hence dispensable so that tissue-specific expression or acquisition of novel biochemical functions may create evolutionary pressure that prevents duplicated genes from becoming inactivated by mutations (see [28] for references). Since the tissue-expression profiles of EBP and EBPL are overlapping and EBP is, as EBPL, ubiquitiously expressed, it is conceivable that EBPL took over an as-yet-unidentified novel biochemical function instead of 3β hydroxysteroid sterol Δ^8-Δ^7 isomerization. So far, redundancy has not been observed for other enzymes of post-squalene sterol metabolism except for the lamin B receptor and TM7SF2, which both reportedly have Δ^{14}-sterol reductase activity [29,30].

Lack of catalytic activity of EBPL in yeast is unexpected and intriguing, considering that 9 out of 10 amino acid residues which are essential for EBP-mediated catalysis [16] are conserved in EBPL. Attempts to restore enzymic activity by a single amino acid substitution or chimaerization failed, indicating that no single amino acid substitution is responsible for the lack of 3β-hydroxysteroid sterol Δ^8-Δ^7 isomerase activity of EBPL. Structural similarity and conservation of amino acid residues, but lack of enzymic activity, suggested that EBPL might only function in association with EBP. In this model, EBP would be active by itself, as is evident from its ability to complement the 3β-hydroxysteroid sterol Δ^8-Δ^7 isomerase-deficient yeast strain WA0 but would acquire additional properties by associating with EBPL. Similar amounts of EBP and EBPL in hepatic microsomes supported the idea of stoichiometric heterodimerization while different distributions of the mRNA and lack of co-regulation of expression (see below) argued against this possibility. A prerequisite for EBP and EBPL being part of a functional complex would be that EBP and EBPL physically interact. We investigated the interaction between EBP and EBPL using recombinant epitope-tagged proteins expressed in human embryonic kidney cells (tsA201). These cells endogenously expressed EBP and EBPL, indicating that they have the molecular machinery for correct targeting of both proteins. αEBPL serum specifically and quantitatively precipitated EBPL, but co-immunoprecipitated only a small fraction of EBP. Next we reasoned that if EBP–EBPL interactions could be not detected by immunoprecipitation glutaraldehyde cross-linking could reveal whether EBP associated with itself or EBPL. Cross-linked dimers containing either EBP or EBPL differed in their migration in SDS/PAGE, indicating that EBP and EBPL were not part of the same cross-linked complex. We cannot rule out that these homomeric EBP–EBP and EBPL–EBPL complexes interact weakly with each other.

If EBPL was an enzyme of sterol metabolism, its mRNA would be up-regulated upon inhibition of sterol biosynthesis. We therefore investigated the effect of mevinolin, an inhibitor of HMG-CoA reductase, the key enzyme of sterol metabolism, on steady-state EBPL mRNA levels in HepG2 cells. This treatment induced EBP and DHCR7 mRNAs as reported previously [26,27] but failed to increase the mRNAs for EBPL and sigma$_1$ receptor. This indicates that transcription of EBP and EBPL are not co-ordinately regulated and suggests that EBPL, similar to the sigma$_1$ receptor, functions outside of sterol biosynthesis.

Our work identified and characterized EBPL, a novel microsomal protein that has neither detectable 3β-hydroxysteroid sterol Δ^8-Δ^7 isomerase nor sigma-ligand-binding activity when expressed in yeast, despite a distant evolutionary relationship with EBP, the vertebrate 3β-hydroxysteroid sterol Δ^8-Δ^7 isomerase. Therefore EBPL is not the long-sought sigma$_2$-receptor. Endogenous EBPL forms homodimers upon chemical cross-linking.

In contrast with EBP, EBPL expression is not sterol-responsive, suggesting that EBPL is not an enzyme of sterol metabolism. We therefore propose that EBPL has a yet-to-be-determined novel biological function. Like the lamin B receptor and the sigma$_1$ receptor, EBPL is a member of a group of genes which originated from enzymes of sterol metabolism and acquired novel biological functions while either preserving (lamin B receptor) or losing (sigma$_1$ receptor, EBPL) their original catalytic activity.

This work was supported by grants from Fonds zur Förderung der Wissenschaftlichen Forschung (P14112 to H. G.), the Österreichische Nationalbank (ÖNB-8303 to H. G.) and the Legerlotz foundation (to F. F. M.). We thank B. Fiechtner and S. Geiger for excellent technical assistance and J. Striessnig for helpful comments.

REFERENCES

1 Moebius, F. F., Striessnig, J. and Glossmann, H. (1997) The mysteries of sigma-receptors: new family members reveal a role in cholesterol synthesis. Trends Pharmacol. Sci. **18**, 67–70
2 Silve, S., Dupuy, P. H., Labit-Lebouteiller, C., Kaghad, M., Chalon, P., Rahier, A., Taton, M., Lupker, J., Shire, D. and Loison, G. (1996) Emopamil-binding protein, a mammalian protein that binds a series of structurally diverse neuroprotective agents, exhibits Δ^8-Δ^7 isomerase activity in yeast. J. Biol. Chem. **271**, 22434–22440
3 Hayashi, T. and Su, T. P. (2001) Regulating ankyrin dynamics: roles of sigma-1 receptors. Proc. Natl. Acad. Sci. U.S.A. **98**, 491–496
4 Aydar, E., Palmer, C. P., Klyachko, V. A. and Jackson, M. B. (2002) The sigma receptor as a ligand-regulated auxiliary potassium channel subunit. Neuron **34**, 399–410
5 Moebius, F. F., Reiter, R. J., Bermoser, K., Glossmann, H., Cho, S. Y. and Paik, Y. K. (1998) Pharmacological analysis of sterol Δ^8-Δ^7 isomerase proteins with [^{3}H]ifenprodil. Mol. Pharmacol. **54**, 591–598
6 Liu, X. Y., Dangel, A. W., Kelley, R. I., Zhao, W., Denny, P., Botcherby, M., Cattanach, B., Peters, J., Hunsicker, P. R., Mallon, A. M. et al. (1999) The gene mutated in bare patches and striated mice encodes a novel 3β-hydroxysteroid dehydrogenase. Nat. Genet. **22**, 182–187
7 Braverman, N., Lin, P., Moebius, F. F., Obie, C., Moser, A., Glossmann, H., Wilcox, W. R., Rimoin, D. L., Smith, M., Kratz, L. et al. (1999) Mutations in the gene encoding 3β-hydroxysteroid-Δ^8, Δ^7-isomerase cause X-linked dominant Conradi-Hunermann syndrome. Nat. Genet. **22**, 291–294
8 Aughton, D. J., Kelley, R. I., Metzenberg, A., Pureza, V. and Pauli, R. M. (2003) X-linked dominant chondrodysplasia punctata (CDPX2) caused by single gene mosaicism in a male. Am. J. Med. Genet. **116**, 255–260
9 Milunsky, J. M., Maher, T. A. and Metzenberg, A. B. (2003) Molecular, biochemical, and phenotypic analysis of a hemizygous male with a severe atypical phenotype for X-linked dominant Conradi-Hunermann-Happle syndrome and a mutation in EBP. Am. J. Med. Genet. **116**, 249–254
10 Herman, G. E. (2000) X-linked dominant disorders of cholesterol biosynthesis in man and mouse. Biochim. Biophys. Acta **1529**, 357–373
11 Hellewell, S. B., Bruce, A., Feinstein, G., Orringer, J., Wiliams, W. and Bowen, W. D. (1994) Rat liver and kidney contain high densities of sigma1 and sigma2 receptors: characterization by ligand binding and photoaffinity labeling. Eur. J. Pharmacol. **268**, 9–18
12 Kyte, J. and Doolittle, R. F. (1982) A simple method for displaying the hydropathic character of a protein. J. Mol. Biol. **157**, 105–132
13 Kelley, R. I. (1995) Diagnosis of Smith-Lemli-Opitz syndrome by gas chromatography/mass spectrometry of 7-dehydrocholesterol in plasma, amniotic fluid and cultured skin fibroblasts. Clin. Chim. Acta **236**, 45–58
14 Hanner, M., Moebius, F. F., Weber, F., Grabner, M., Striessnig, J. and Glossmann, H. (1995) Phenylalkylamine Ca^{2+} antagonist binding protein. Molecular cloning, tissue distribution, and heterologous expression. J. Biol. Chem. **270**, 7551–7557
15 Fitzky, B. U., Witsch-Baumgartner, M., Erdel, M., Lee, J. N., Paik, Y.-K., Glossmann, H., Utermann, G. and Moebius, F. F. (1998) Mutations in the Δ^7-sterol reductase gene in patients with the Smith-Lemli-Opitz syndrome. Proc. Natl. Acad. Sci. U.S.A. **95**, 8181–8186
16 Moebius, F. F., Soellner, K. E., Fiechtner, B., Huck, C. W., Bonn, G. and Glossmann, H. (1999) Histidine77, glutamic acid81, glutamic acid123, threonine126, asparagine194, and tryptophan197 of the human emopamil binding protein are required for *in vivo* sterol Δ^8-Δ^7 isomerization. Biochemistry **38**, 1119–1127
17 Moebius, F. F., Hanner, M., Knaus, H.-G., Weber, F., Striessnig, J. and Glossmann, H. (1994) Purification and N-terminal sequencing of the high affinity phenylalkylamine Ca^{2+} antagonist binding protein from guinea-pig liver endoplasmic reticulum. J. Biol. Chem. **269**, 29314–29320
18 Hanner, M., Moebius, F. F., Flandorfer, A., Knaus, H.-G., Striessnig, J., Kempner, E. and Glossmann, H. (1996) Purification, molecular cloning, and expression of the mammalian sigma$_1$ binding site. Proc. Natl. Acad. Sci. U.S.A. **93**, 8072–8077
19 Jackson, M. R., Nilsson, T. and Peterson, P. A. (1990) Identification of motifs for retention of transmembrane proteins in the endoplasmic reticulum. EMBO J. **9**, 3153–3162
20 Grebenok, R. J., Ohnmeiss, T. E., Yamamoto, A., Huntley, E. D., Galbraith, D. W. and Della, P. D. (1998) Isolation and characterization of an *Arabidopsis thaliana* C-8,7 sterol isomerase: functional and structural similarities to mammalian C-8,7 sterol isomerase/emopamil-binding protein. Plant Mol. Biol. **38**, 807–815
21 Felsenstein, J. (1997) An alternating least squares approach to inferring phylogenies from pairwise distances. Syst. Biol. **46**, 101–111
22 Hedges, S. B. (2002) The origin and evolution of model organisms. Nat. Rev. Genet. **3**, 838–849
23 Zhang, M. Q. (1998) Statistical features of human exons and their flanking regions. Hum. Mol. Genet. **7**, 919–932
24 Ashman, W. H., Barbuch, R. J., Ulbright, C. E., Jarrett, H. W. and Bard, M. (1991) Cloning and disruption of the yeast C-8 sterol isomerase gene. Lipids **26**, 628–632
25 Dussossoy, D., Carayon, P., Belugou, S., Feraut, D., Bord, A., Goubet, C., Roque, C., Vidal, H., Combes, T., Loison, G. and Casellas, P. (1999) Colocalization of sterol isomerase and sigma$_1$ receptor at endoplasmic reticulum and nuclear envelope level. Eur. J. Biochem. **263**, 377–386
26 Kim, J. H., Lee, J. N. and Paik, Y. K. (2001) Cholesterol biosynthesis from lanosterol. A concerted role for Sp1 and NF-Y-binding sites for sterol-mediated regulation of rat 7-dehydrocholesterol reductase gene expression. J. Biol. Chem. **276**, 18153–18160
27 Bae, S., Seong, J. and Paik, Y. (2001) Cholesterol biosynthesis from lanosterol: molecular cloning, chromosomal localization, functional expression and liver-specific gene regulation of rat sterol Δ^8-isomerase, a cholesterogenic enzyme with multiple functions. Biochem. J. **353**, 689–699
28 Gogarten, J. P. and Olendzenski, L. (1999) Orthologs, paralogs and genome comparisons. Curr. Opin. Genet. Dev. **9**, 630–636
29 Silve, S., Dupuy, P. H., Ferrara, P. and Loison, G. (1998) Human lamin B receptor exhibits sterol C14-reductase activity in *Saccharomyces cerevisiae*. Biochim. Biophys. Acta **1392**, 233–244
30 Roberti, R., Bennati, A. M., Galli, G., Caruso, D., Maras, B., Aisa, C., Beccari, T., Della Fazia, M. A. and Servillo, G. (2002) Cloning and expression of sterol Δ^{14}-reductase from bovine liver. Eur. J. Biochem. **269**, 283–290

Received 26 March 2003/30 April 2003; accepted 21 May 2003
Published as BJ Immediate Publication 21 May 2003, DOI 10.1042/BJ20030465